

Quantum walk search for exceptional configurations

Pulak Ranjan Giri*

KDDI Research, Inc., Fujimino-shi, Saitama, Japan

(Dated: July 4, 2025)

There exist two types of configurations of marked vertices on a two-dimensional grid, known as the *exceptional configurations*, which are hard to find by the discrete-time quantum walk algorithms. In this article, we provide a comparative study of the quantum walk algorithm with different coins to search these *exceptional configurations* on a two-dimensional grid. We further extend the analysis to the hypercube, where only one type of *exceptional configurations* are present. Our observation, backed by numerical results, is that our recently proposed modified coin operator is the only coin which can search both types of *exceptional configurations* as well as non-*exceptional configurations* successfully. As a consequence, we observe that the existence of *exceptional configurations* are not a quantum phenomenon, rather a mere limitation of some of the coin operators.

PACS numbers: 03.67.Ac, 03.67.Lx, 03.65.-w

I. INTRODUCTION

Searching a database is one of the important tasks in many applications of computer science. Given an unsorted database of size N , a classical computer takes $\mathcal{O}(N)$ time to find out a specific element from the database in the worst case scenario. However, quantum computer can do the same job faster [1] than the classical computer, because it can exploit quantum superposition in its favour. Grover's quantum search algorithm [2] can search for a marked element in the database quadratically faster, in $\mathcal{O}(\sqrt{N})$ time. A detailed review on Grover's search algorithm and its generalizations is presented in ref. [3].

Generalization of the Grover's search to the quantum search on graph is not straightforward. Searching on graphs is subject to the constraint that we are only allowed to shift from one vertex of the graph to only the nearest neighbour vertices in one time step. Although Grover search requires $\mathcal{O}(\sqrt{N})$ iterations, but each iteration needs another $\mathcal{O}(\sqrt{N})$ time to perform all the reflections, making the total time $\mathcal{O}(N)$ [4].

In this regard, quantum walk [5], which is the quantum counterpart of the classical random walk, has been very much successful in searching on graphs faster than the classical exhaustive search. Both continuous- [6] and discrete-time [7] quantum walk can be exploited to search for the marked vertices on a graph. Some of the examples of the quantum walk search include searching on one- [8, 9], two- [10] and more than two-dimensional grid [11] with periodic boundary conditions and many other graphs [12, 13] as well. Specifically, on two-dimensional grid Grover's algorithm together with multi-level recursion [14] can search for a marked vertex in $\mathcal{O}(\sqrt{N} \log^2 N)$ time. The discrete-time quantum walk can perform the same search in $\mathcal{O}(\sqrt{N} \log N)$ time with a possible improvement of $\mathcal{O}(\sqrt{\log N})$ [15] by some addi-

tional techniques. However, lackadaisical quantum walk [16–18] can directly search on the two-dimensional grid in $\mathcal{O}(\sqrt{N \log N})$ time without the help of any additional technique. Optimal speed of $\mathcal{O}(\sqrt{\frac{N}{M}})$ can be achieved by lackadaisical quantum walk search [19] if additional long range edges of a specific type are attached with the two-dimensional grid. In continuous-time quantum walk, optimal speed of $\mathcal{O}(\sqrt{N})$ for a single vertex search has been achieved [20] by adding long range edges to the two-dimensional grid.

In discrete-time quantum walk, marked vertices are distinguished from the unmarked vertices by modifying the coin operator. SKW coin, \mathcal{C}_{SKW} , [21] and Grover coin, \mathcal{C}_{Grover} , [14] are two such widely used modified coins, which differentiate marked vertices from the unmarked vertices. For example, SKW coin based quantum walk search algorithm applies Grover diffusion operator, D_0 , to the unmarked vertices and $-\mathbb{I}$ to the marked vertices. Whereas, Grover coin based quantum walk algorithm applies D_0 to the unmarked vertices and $-D_0$ to the marked vertices. Search algorithms based on these two coins have been very much successful in finding a single marked vertex on a graph. However, while searching for multiple marked vertices [22–24] there are certain limitations to the search problem. For example, Grover coin can not find two adjacent marked vertices [25] on a two-dimensional periodic lattice. Also, the set of marked vertices, arranged in a $2k \times m$ or $k \times 2m$ block for any positive k and m , can not be found. However, for the set of marked vertices arranged in a $k \times m$ block for k and m both being odd, Grover coin can be used to search any of the marked vertices in these blocks. On the other hand, marked vertices, arranged along the diagonal of a two-dimensional grid and its certain generalised configurations [26, 27], can not be searched using SKW coin. Such configurations of marked vertices on the two-dimensional grid as well as on some other graphs, which can not be found by the SKW and/or Grover coin, are collectively known as the *exceptional configurations*.

To overcome the limitations of the SKW and Grover

* pu-giri@kddi-research.jp

coin, recently a coin operator, \mathcal{C}_G , is proposed by us in ref. [28], which is obtained by modifying the coin operator, \mathcal{C}_l , of the lackadaisical quantum walk search. Instead of flipping the sign of all the basis states of the marked vertices it only flips the sign of the self-loop attached to the marked vertices followed by the Grover diffusion operator acting on the coin basis states of the marked vertices. Quantum walk search then effectively becomes a Grover search for the self-loops of the marked vertices. This coin can search the *exceptional configurations* as well as any other type of configurations of the marked vertices.

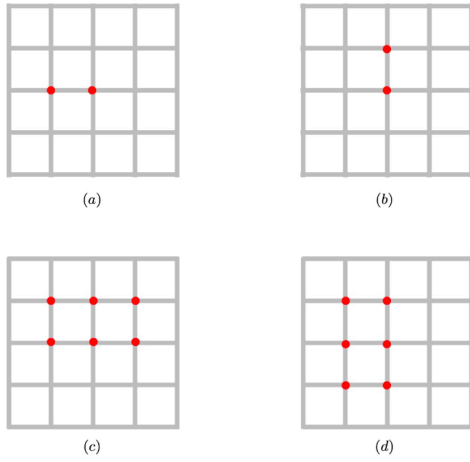


FIG. 1: Two-dimensional grid with periodic boundary conditions: a pair of marked vertices in (a) horizontal direction, and in (b) vertical direction; and a cluster of marked vertices of the form (c) $k \times 2m$ and (d) $2k \times m$, for k, m being positive integers.

It has been seen that, mostly SKW, Grover coin and coin for the lackadaisical quantum walk search, \mathcal{C}_l , have difficulty in finding the *exceptional configurations* of marked vertices. However, adding more marked vertices makes the classical search problem easier by making the search time less and success probability more. Based on this observation, it was suggested in refs. [25, 29] that the occurrence of the *exceptional configurations* are a quantum phenomenon.

In this article a comparative study on the performance of quantum walk algorithm with different coin operators to search *exceptional configurations* shows that, the occurrence of *exceptional configurations* are merely the limitation of some of the coin operators, which can be overcome by a suitably modified coin operator and therefore not a quantum phenomenon. We show that the stationary state [29], which is responsible for the failure to search *exceptional configurations* of a specific type by the Grover coin, actually does not remain stationary under \mathcal{C}_{SKW} and \mathcal{C}_G coins. For the diagonal and its generalised form of *exceptional configurations*, we show that \mathcal{C}_l and \mathcal{C}_G can successfully search the marked vertices in these configurations. We have also studied the quantum walk search for *exceptional configurations* on a hypercube. Experimental

results presented in this article show that \mathcal{C}_G outperforms rest of coin operators discussed in this article.

We arrange this article in the following fashion: A brief discussion on the quantum walk search on a two-dimensional periodic lattice is presented in section II. Then *exceptional configurations* and their quantum walk search algorithm are discussed in section III. Quantum walk search for the *exceptional configurations* on the hypercube is discussed in section IV and finally we conclude in section V.

II. QUANTUM WALK SEARCH ON TWO-DIMENSIONAL GRID

In this section, we provide a brief discussion on the discrete-time quantum walk search algorithm on a two-dimensional grid of size $\sqrt{N} \times \sqrt{N}$ with periodic boundary conditions. Each vertex has four standard edges represented by the basis states $|c_x^+\rangle, |c_x^-\rangle, |c_y^+\rangle, |c_y^-\rangle$ of the coin space. Hilbert space of the graph, $\mathcal{H}_G = \mathcal{H}_C \otimes \mathcal{H}_V$, is the tensor product of the coin, \mathcal{H}_C , and vertex, \mathcal{H}_V , space respectively. Quantum walk search starts with the initial state, $|\psi_{in}\rangle = |\psi_c\rangle \otimes |\psi_v\rangle$, prepared with the uniform superposition of all the basis states on both coin and vertex spaces respectively as

$$|\psi_c\rangle = \frac{1}{\sqrt{4}} (|c_x^+\rangle + |c_x^-\rangle + |c_y^+\rangle + |c_y^-\rangle), \quad (1)$$

$$|\psi_v\rangle = \frac{1}{\sqrt{N}} \sum_{v_x, v_y=0}^{\sqrt{N}-1} |v_x, v_y\rangle. \quad (2)$$

Time evolution operator \mathcal{U} then acts on the initial state $|\psi_{in}\rangle$ repeatedly until the final state

$$|\psi_f\rangle = \mathcal{U}^t |\psi_{in}\rangle, \quad (3)$$

has high fidelity with the state representing the marked vertices. Usually, in the lackadaisical quantum walk the final state $|\psi_f\rangle$ directly reaches to the state for the marked vertex. However, in quantum walk search without self-loop, final state does not have high overlap with the state of marked vertex. So, we need amplitude amplification technique to achieve high and constant success probability.

The time evolution operator in the quantum walk search algorithm is composed of the coin operator \mathcal{C} followed by the flip-flop shift operator S as

$$\mathcal{U} = SC. \quad (4)$$

Depending on how the coin operator acts on the marked and unmarked vertices, it can be given a general form

$$\mathcal{C} = C_+ \otimes \left(\mathbb{I}_{N \times N} - \sum_{i=1}^M |t_i\rangle\langle t_i| \right) + C_- \otimes \sum_{i=1}^M |t_i\rangle\langle t_i|, \quad (5)$$

where C_+ and C_- act on the unmarked and marked vertices respectively and t_i s are the marked vertices. Two

of the well known coin operators obtained from eq. (5) are the following

$$\mathcal{C}_{Grover} = D_0 \otimes \left(\mathbb{I}_{N \times N} - 2 \sum_{i=1}^M |t_i\rangle\langle t_i| \right), \quad (6)$$

$$\mathcal{C}_{SKW} = D_0 \otimes \left(\mathbb{I}_{N \times N} - \sum_{i=1}^M |t_i\rangle\langle t_i| \right) - \mathbb{I}_{4 \times 4} \otimes \sum_{i=1}^M |t_i\rangle\langle t_i|, \quad (7)$$

where the Grover coin, \mathcal{C}_{Grover} , is obtained by replacing $C_+ = -C_- = D_0 = 2|\psi_c\rangle\langle\psi_c| - \mathbb{I}_{4 \times 4}$ and the SKW coin, \mathcal{C}_{SKW} , is obtained by replacing $C_+ = D_0$, $C_- = -\mathbb{I}$ in eq. (5). Shenvi et al. [21] first used \mathcal{C}_{SKW} coin to search for a marked vertex on a hypercube in optimum time. Both of the coins in eq. (6) and (7) have been used in ref. [7] to study spatial search on a two and higher dimensional grid, hypercube and on a complete graph. Note that these two coins have been referred to as Grover and AKR coins of the AKR algorithm respectively in ref. [25]. Previously, we referred Grover coin as AKR coin in [28], because it has been used by AKR [7] to search for a marked vertex on a complete graph.

Quantum walk can be generalised to lackadaisical quantum walk by adding a self-loop state $|c_l\rangle$ with weight l to each vertex of the graph. Then the coin operator for the lackadaisical quantum walk search is given by

$$\mathcal{C}_l = D_l \otimes \left(\mathbb{I}_{N \times N} - 2 \sum_{i=1}^M |t_i\rangle\langle t_i| \right), \quad (8)$$

where the Grover diffusion operator $D_l = 2|\psi_c^l\rangle\langle\psi_c^l| - \mathbb{I}_{5 \times 5}$ can be obtained from the initial state

$$|\psi_c^l\rangle = \frac{1}{\sqrt{4+l}} \left(|c_x^+\rangle + |c_x^-\rangle + |c_y^+\rangle + |c_y^-\rangle + \sqrt{l}|c_l\rangle \right). \quad (9)$$

Note that regular quantum walk can be obtained from lackadaisical quantum walk by setting $l = 0$. Usually, we need to find out an optimal value for the self-loop weight l for which the success probability is maximised. However, in this article we will only choose a suitable value for the self-loop weight such that we have a reasonably high success probability to carry out our analysis on *exceptional configurations*.

To overcome the limitations of the above mentioned coin operators in searching for the *exceptional configurations* of marked vertices, we recently proposed [28] the following modified coin

$$\mathcal{C}_G = (D_l \otimes \mathbb{I}_{N \times N}) \left(\mathbb{I}_{5 \times 5} \otimes \mathbb{I}_{N \times N} - 2 \sum_{i=1}^M |c_l, t_i\rangle\langle c_l, t_i| \right). \quad (10)$$

After the coin operation, the flip-flop shift operator acts

on the basis states of the vertex space as

$$S|c_x^+\rangle|v_x; v_y\rangle = |c_x^-\rangle|v_x + 1; v_y\rangle, \quad (11)$$

$$S|c_x^-\rangle|v_x; v_y\rangle = |c_x^+\rangle|v_x - 1; v_y\rangle, \quad (12)$$

$$S|c_y^+\rangle|v_x; v_y\rangle = |c_y^-\rangle|v_x; v_y + 1\rangle, \quad (13)$$

$$S|c_y^-\rangle|v_x; v_y\rangle = |c_y^+\rangle|v_x; v_y - 1\rangle, \quad (14)$$

$$S|c_l\rangle|v_x; v_y\rangle = |c_l\rangle|v_x; v_y\rangle. \quad (15)$$

The success probability to find the marked vertices becomes

$$p_{succ} = \sum_{i=1}^M |\langle t_i | U^t | \psi_{in}^l \rangle|^2, \quad (16)$$

where sum over coin basis states is also done at the marked vertices.

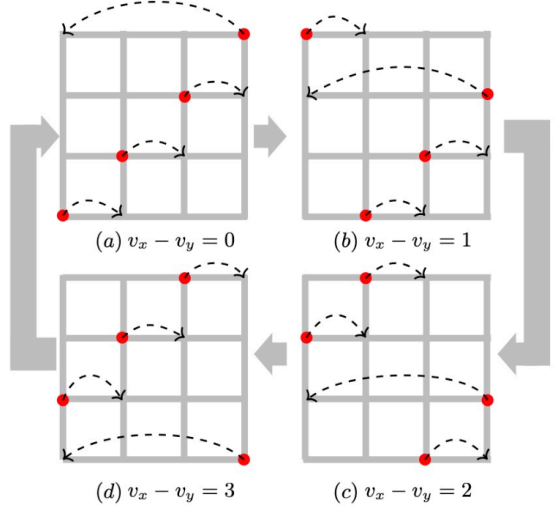


FIG. 2: Two-dimensional grid with periodic boundary conditions with *exceptional configurations* of the form (a) – (d) $i - j = \text{const.}$

III. EXCEPTIONAL CONFIGURATIONS

As stated in the introduction, there are *exceptional configurations* of marked vertices in the two-dimensional grid and in other graphs, for which the success probability to measure the marked vertices does not improve despite repeated application of the iteration operator of the quantum walk search algorithm. Two types of *exceptional configurations*, let us denote them as *I* and *II*, are reported in the literature [25–27]. In this section we will discuss these configurations in detail and show how we can search these configurations by a suitably modified coin operator. We also discuss the existence of stationary states with very high overlap with the initial state of uniform superposition of all the basis states, which is

responsible for the failure to find *exceptional configurations I* by the Grover coin based quantum walk search algorithm.

A. Exceptional configurations I

These type of *exceptional configurations* occur when two marked vertices are adjacent to each other. Fig. 1 (a) and (b) are examples of two pairs of adjacent marked vertices located in horizontal and vertical directions respectively. More generally, group of marked vertices of the form $k \times 2m$ and $2k \times m$, for k, m being positive integers, are *exceptional configurations* on a two-dimensional grid, which the Grover coin can not find. Fig 1(c) and (d), with marked vertices of the form 3×2 and 2×3 respectively, are examples of such general configurations.

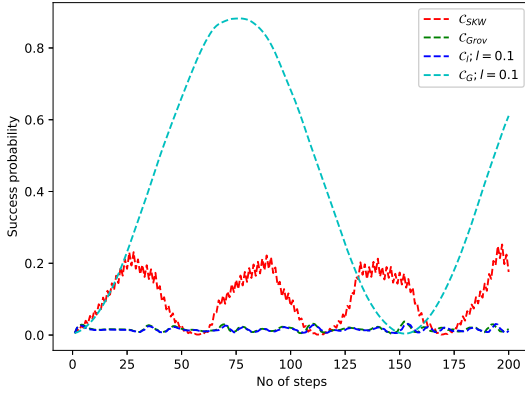


FIG. 3: Success probability to measure a randomly chosen pair of adjacent marked vertices in horizontal direction (*exceptional configurations I*) on a 20×20 square grid as a function of the number of iteration steps for four different coin operators.

1. Stationary state

We are interested in the stationary state, which has large overlap with the initial state of the quantum walk search. For a detailed analysis on how to construct the stationary state and use it in the quantum walk search to show that the success probability of the adjacent vertices remains close to their initial success probability see refs. [23, 25, 29]. To summarise the result for our purpose, let us consider a pair of adjacent marked vertices on a $\sqrt{N} \times \sqrt{N}$ square lattice. These two marked vertices can either be in horizontal direction as (i, j) and $(i+1, j)$ or in vertical direction as (i, j) and $(i, j+1)$, where i and j are the coordinates representing horizontal and vertical directions respectively. Since we are looking for a stationary state, which is very close to the uniform superposition of basis states, we assume that all the vertices, except the marked ones, have the coin state of the

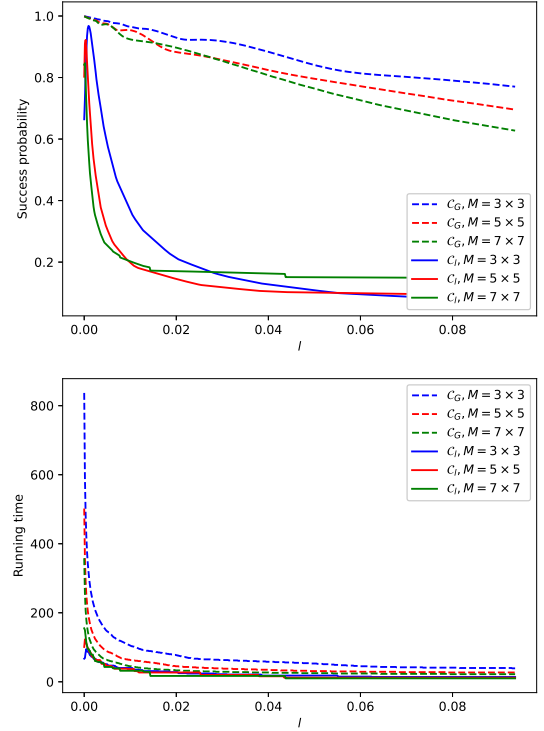


FIG. 4: Success probability (top) and running time (bottom) to search marked vertices of the block form $k \times m$, k, m being odd, as a function of the self-loop weight l for a 20×20 square grid.

form in eq. (9). However for the pair of marked vertices in the horizontal direction we need the following pair of non-normalized coin states

$$|\psi_c^{x+}\rangle = |\psi_c^l\rangle - \sqrt{4+l}|c_x^+\rangle \quad (17)$$

$$|\psi_c^{x-}\rangle = |\psi_c^l\rangle - \sqrt{4+l}|c_x^-\rangle. \quad (18)$$

Similarly, for the pair of marked vertices in the vertical direction we need the following pair of non-normalized coin states

$$|\psi_c^{y+}\rangle = |\psi_c^l\rangle - \sqrt{4+l}|c_y^+\rangle \quad (19)$$

$$|\psi_c^{y-}\rangle = |\psi_c^l\rangle - \sqrt{4+l}|c_y^-\rangle. \quad (20)$$

Note that, the above four states are orthogonal to $|\psi_c^l\rangle$, i.e., $\langle\psi_c^{x+}|\psi_c^l\rangle = \langle\psi_c^{x-}|\psi_c^l\rangle = \langle\psi_c^{y+}|\psi_c^l\rangle = \langle\psi_c^{y-}|\psi_c^l\rangle = 0$.

Case 1: The stationary state in this case has all the unmarked vertices with coin state of the form $|\psi_c^l\rangle$ and the two horizontal marked vertices (i, j) and $(i+1, j)$ with their coin states of the form $|\psi_c^{x+}\rangle$ and $|\psi_c^{x-}\rangle$ respectively. Specifically, the stationary state has the following form

$$|\psi_{hstat}\rangle = |\psi_{in}^l\rangle - \sqrt{\frac{4+l}{N}} (|c_x^+\rangle \otimes |i, j\rangle + |c_x^-\rangle \otimes |i+1, j\rangle), \quad (21)$$

where the initial state $|\psi_{in}^l\rangle = |\psi_c^l\rangle \otimes |\psi_v\rangle$.

Case 2: Similarly, in the vertical case, the stationary state has the following form

$$|\psi_{vstat}\rangle = |\psi_{in}^l\rangle - \sqrt{\frac{4+l}{N}} (|c_y^+\rangle \otimes |i, j\rangle + |c_y^-\rangle \otimes |i, j+1\rangle). \quad (22)$$

U_l : It has been shown in ref. [23] that these two types of states $|\psi_{hstat}\rangle$ and $|\psi_{vstat}\rangle$ are eigenstates of the evolution operator of lackadaisical quantum walk, $U_l = S\mathcal{C}_l$, with unit eigenvalue:

$$U_l|\psi_{hstat}\rangle = |\psi_{hstat}\rangle, \quad (23)$$

$$U_l|\psi_{vstat}\rangle = |\psi_{vstat}\rangle. \quad (24)$$

U_{Groves} : These two states $|\psi_{hstat}\rangle$ and $|\psi_{vstat}\rangle$ remain eigenstates [25] for the regular quantum walk search with Grover coin, $U_{Groves} = U_{l=0}$,

$$U_{Groves}|\psi_{hstat}\rangle_{l=0} = |\psi_{hstat}\rangle_{l=0}, \quad (25)$$

$$U_{Groves}|\psi_{vstat}\rangle_{l=0} = |\psi_{vstat}\rangle_{l=0}. \quad (26)$$

U_G : However, under $U_G = S\mathcal{C}_G$, the stationary states do not remain stationary as can be seen from the following expressions

$$U_G|\psi_{hstat}\rangle = |\psi_{hstat}\rangle - \frac{2}{\sqrt{N}} S (|\psi_c^{x+}\rangle \otimes |i, j\rangle + |\psi_c^{x-}\rangle \otimes |i+1, j\rangle) - 2\sqrt{\frac{l}{N(4+l)}} SD_l |l\rangle \otimes (|i, j\rangle + |i+1, j\rangle) \quad (27)$$

$$U_G|\psi_{vstat}\rangle = |\psi_{vstat}\rangle - \frac{2}{\sqrt{N}} S (|\psi_c^{y+}\rangle \otimes |i, j\rangle + |\psi_c^{y-}\rangle \otimes |i, j+1\rangle) - 2\sqrt{\frac{l}{N(4+l)}} SD_l |l\rangle \otimes (|i, j\rangle + |i, j+1\rangle) \quad (28)$$

U_{SKW} : Under $U_{SKW} = S\mathcal{C}_{SKW}$ also the stationary states do not remain stationary as can be seen from the following expressions

$$U_{SKW}|\psi_{hstat}\rangle = |\psi_{hstat}\rangle - \frac{2}{\sqrt{N}} S (|\psi_c^{x+}\rangle \otimes |i, j\rangle + |\psi_c^{x-}\rangle \otimes |i+1, j\rangle) \quad (29)$$

$$U_{SKW}|\psi_{vstat}\rangle = |\psi_{vstat}\rangle - \frac{2}{\sqrt{N}} S (|\psi_c^{y+}\rangle \otimes |i, j\rangle + |\psi_c^{y-}\rangle \otimes |i, j+1\rangle) \quad (30)$$

Note that, for the quantum walk search with SKW coin there is no self-loop state, so we need to set $|c_l\rangle = 0$ and $l = 0$ wherever necessary.

2. Searching adjacent vertices

We can express the initial state $|\psi_{in}^l\rangle$ in terms of the stationary state $|\psi_{hstat}\rangle$ as

$$|\psi_{in}^l\rangle = |\psi_{hstat}\rangle + \sqrt{\frac{4+l}{N}} (|c_x^+\rangle \otimes |i, j\rangle + |c_x^-\rangle \otimes |i+1, j\rangle). \quad (31)$$

The final state, after applying U_l repeatedly t times, becomes

$$U_l^t |\psi_{in}^l\rangle = |\psi_{hstat}\rangle + \sqrt{\frac{4+l}{N}} U_l^t (|c_x^+\rangle \otimes |i, j\rangle + |c_x^-\rangle \otimes |i+1, j\rangle). \quad (32)$$

Note that, first part of the right hand side of eq. (32) does not change, only the second part changes under the action of the evolution operator. The amplitude shifts away from the marked vertex pair after each application of the evolution. The upper bound of the probability of marked vertices can be obtained by setting $U_l^t = -\mathbb{I}$ on the second term. Therefore, success probability of the marked vertices is bounded as $p_{succ} \leq \mathcal{O}(1/N)$. Note, this bound also holds for U_{Groves} . The same conclusion can be drawn by taking the other stationary state $|\psi_{vstat}\rangle$ as well. It implies that the quantum walk search by U_l and U_{Groves} on a two-dimensional grid can not find the adjacent vertices, because the success probability remains bounded by the initial success probability. The general configurations of the form $k \times 2m$ and $2k \times m$, for k, m being positive integers, can be obtained by tiling with basic forms 2×1 and 1×2 , also can not be found by U_l and U_{Groves} as well.

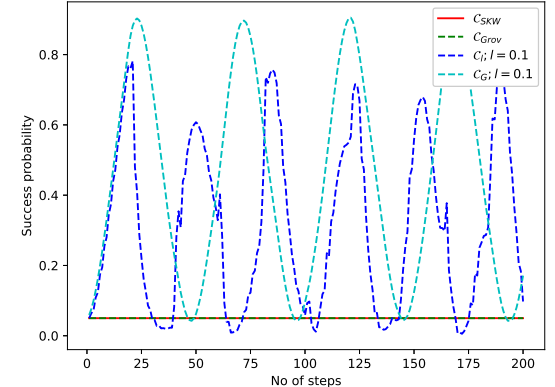


FIG. 5: Success probability to measure the diagonal marked vertices (*exceptional configurations II*) on a 20×20 square grid as a function of the number of iteration steps for four different coin operators.

However, under the action of U_G on the initial state both parts of the initial state in eq. (31) transform non-trivially, since $|\psi_{hstat}\rangle$ is no longer an eigenstate of U_G . After repeated application of the evolution operator the

final state has significantly high and constant overlap with the marked vertices.

For U_{SKW} also both parts of the initial state transform non-trivially. However, to obtain high success probability we need to exploit amplitude amplification in addition to repeated application of U_{SKW} .

Experimental results: The behaviour of the success probability to measure a randomly chosen pair of adjacent marked vertices in the horizontal direction on a 20×20 square lattice as a function of the number of iteration steps has been presented in fig. 3. We see that the success probability for the \mathcal{C}_{Groves} and \mathcal{C}_l coin represented by the green and blue dashed curves do not grow at all even if we increase the number of iteration steps. For the \mathcal{C}_G and \mathcal{C}_{SKW} coin success probability grow as a function of the number of iteration steps represented by the cyan and red dashed curves. For the SKW coin, as we can see, the success probability is not significantly high, so we need to further apply amplitude amplification to enhance the success probability. The experiment is repeated for 10 randomly chosen adjacent vertices in the horizontal direction and another 10 randomly chosen adjacent vertices in the vertical direction with the same experimental setting, which agrees with the result reported in fig. 3.

We have also studied the performance of \mathcal{C}_G and \mathcal{C}_l coins to search the block of marked vertices of the form $k \times m$, for k, m being odd. These configurations, which are not *exceptional configurations*, can be searched by the quantum walk algorithm with all the analysed coin operators in this article. From fig. 4(top) we see that the success probability to search marked vertices by the quantum walk algorithm with \mathcal{C}_G coin, given by the blue, red and green dashed lines are much better compared to the quantum walk algorithm with \mathcal{C}_l coin, given by the blue, red and green continuous lines. From the bottom figure we see that running time of \mathcal{C}_G can almost overlap with the standard running time given by \mathcal{C}_l coin by suitably tuning the self-loop weight l without much compromising success probability as the success probability of \mathcal{C}_G coin changes slowing as a function of l . Although \mathcal{C}_{Groves} and \mathcal{C}_{SKW} coins can also search these configurations, we have not included these results in fig. 4, because we need additional amplitude amplifications technique for these two coins to obtain high enough success probability to compare.

B. Exceptional configurations II

Another type of *exceptional configurations* are the marked vertices along the diagonal of a two-dimensional square lattice. In fig. 2(a) red vertices along the diagonal form this configuration, which the SKW coin can not find [26]. It has been shown in ref. [27] that this diagonal configuration is a special case of a more general *exceptional configurations* of the form $i - j = \alpha$, $\alpha = 0, 1, \dots, \sqrt{N} - 1$. Fig. 2(a) - (d) are examples of these general form of

Coin	Excep. configs. I		Excep. configs. II
	Stationary state exists?	Quantum walk search possible?	Quantum walk search possible?
\mathcal{C}_{Groves}	Yes	No	No
\mathcal{C}_{SKW}	No	Yes	No
\mathcal{C}_l	Yes	No	Yes
\mathcal{C}_G	No	Yes	Yes

TABLE I: Comparison of the performance of quantum walk search algorithm with four different coin operators on a two-dimensional grid to search for the *exceptional configurations*.

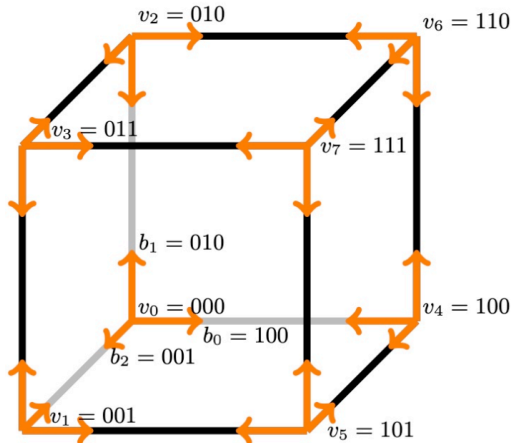


FIG. 6: A $n = 3$ dimensional hypercube with $N = 2^n = 8$ vertices.

exceptional configurations for $\alpha = 0, 1, 2, 3$. Another form of general *exceptional configurations* are of the form $i + j = \alpha$, which can be obtained by rotating the grids in fig. 2(a) - (d) by $\pi/2$. Note that, each configuration in fig. 2 can be obtained from its left fig by translating the marked vertices by one unit to the right as depicted by the fat arrows. Because of the periodicity in square lattice, translating to the left direction also gives the same result.

Consider a $\sqrt{N} \times \sqrt{N}$ grid with all the diagonal vertices being marked. It has been analytically shown in refs. [26, 27] that the success probability to measure the diagonal marked vertices in case of SKW coin remains at its initial value despite repeated application of U_{SKW} . To summarise their results, consider the states of the form

$$|\psi_j^+\rangle = \frac{1}{\sqrt{2\sqrt{N}}} \sum_i (|c_x^-\rangle + |c_y^+\rangle) \otimes |i, i+j\rangle, \quad (33)$$

$$|\psi_j^-\rangle = \frac{1}{\sqrt{2\sqrt{N}}} \sum_i (|c_x^+\rangle + |c_y^-\rangle) \otimes |i, i+j\rangle. \quad (34)$$

Then the initial state $|\psi_{in}\rangle$ of the quantum walk can be

rewritten as

$$|\psi_{in}\rangle = \frac{1}{\sqrt{2\sqrt{N}}} \sum_{j=0}^{\sqrt{N}-1} (|\psi_j^+\rangle + |\psi_j^-\rangle). \quad (35)$$

\mathcal{C}_{SKW} : For $t < \sqrt{N}$, we have

$$U_{SKW}^t \sum_{j=0}^{\sqrt{N}-1} |\psi_j^+\rangle = - \sum_{j=1}^t |\psi_j^-\rangle + \sum_{j=0}^{\sqrt{N}-t-1} |\psi_j^+\rangle, \quad (36)$$

$$U_{SKW}^t \sum_{j=0}^{\sqrt{N}-1} |\psi_j^-\rangle = - \sum_{j=\sqrt{N}-t}^{\sqrt{N}-1} |\psi_j^+\rangle + \sum_{j=t+1}^{\sqrt{N}} |\psi_j^-\rangle. \quad (37)$$

If we apply the evolution operator U_{SKW} to the initial state $|\psi_{in}\rangle$ for a time period of $x\sqrt{N} + t$ we obtain the final state $(-1)^x|\phi^t\rangle$, where

$$|\phi^t\rangle = -|\psi_{in}\rangle + \sqrt{\frac{2}{\sqrt{N}}} \left[\sum_{j=t+1}^{\sqrt{N}} |\psi_j^-\rangle + \sum_{j=0}^{\sqrt{N}-t-1} |\psi_j^+\rangle \right] \quad (38)$$

The second part of eq. (38) becomes zero for $t = \sqrt{N}$. The success probability to measure the marked vertices along the diagonal is $1/\sqrt{N}$. The same result on the success probability can also be obtained for the generalised *exceptional configurations* $j - i = \alpha$ and $i + j = \alpha$ by appropriate translation operation.

\mathcal{C}_{Grover} : Although it has been discussed in the literature that the diagonal configuration and its associated generalised *exceptional configurations* can not be searched by the SKW coin, we find that the same conclusion can be drawn about the Grover coin also. For $t < \sqrt{N}$, we have

$$U_{Grover}^t \sum_{j=0}^{\sqrt{N}-1} |\psi_j^+\rangle = \sum_{j=0}^{\sqrt{N}-t-1} |\psi_j^+\rangle - \sum_{j=\sqrt{N}-t}^{\sqrt{N}-1} |\psi_j^+\rangle \quad (39)$$

$$U_{Grover}^t \sum_{j=0}^{\sqrt{N}-1} |\psi_j^-\rangle = - \sum_{j=1}^t |\psi_j^-\rangle + \sum_{j=t+1}^{\sqrt{N}} |\psi_j^-\rangle. \quad (40)$$

If we apply the evolution operator U_{Grover} to the initial state $|\psi_{in}\rangle$ for a period of time $x\sqrt{N} + t$, we obtain the same final state $(-1)^x|\phi^t\rangle$, which is obtained in SKW coin case.

However, in case of \mathcal{C}_l , \mathcal{C}_G the initial state evolves non-trivially, which allows us to search *exceptional configurations* II with constant success probability.

Experimental results: Behaviour of the success probability to measure the marked vertices along the diagonal, $j - i = 0$, of a 20×20 square grid as a function of the number of iteration steps has been presented in fig. 5. Generalised *exceptional configurations* of the forms $j - i = \alpha$ and $i + j = \alpha$ for all values of α have also been numerically checked for the same experimental setting, which agrees with fig. 5.

We see that the success probability for the \mathcal{C}_{SKW} and \mathcal{C}_{Grover} coins represented by the red and green dashed

curves respectively do not grow at all even if we increase the number of iteration steps. However, for \mathcal{C}_l and \mathcal{C}_G coins the success probability grow as a function of the number of iteration steps represented by the blue and cyan dashed curves respectively.

A summary of performances for four different coin operators to search *exceptional configurations* has been presented in table 1. \mathcal{C}_{Grover} can not find both types of *exceptional configurations*, while \mathcal{C}_{SKW} can not find *exceptional configurations II* and \mathcal{C}_l can not find *exceptional configurations I*. However, \mathcal{C}_G can find both types of *exceptional configurations* with constant success probability.

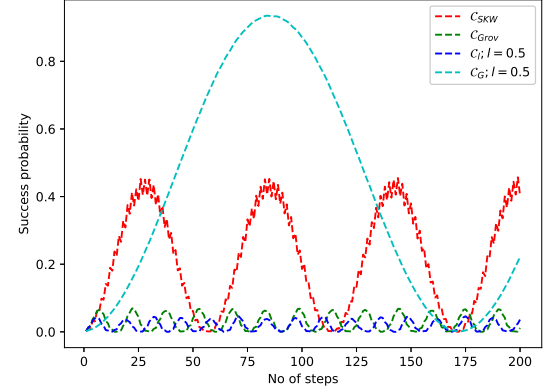


FIG. 7: Success probability of a randomly chosen pair of adjacent marked vertices(*exceptional configuration I*) as a function of the number of iteration steps for a $n = 10$ dimensional hypercube.

IV. QUANTUM WALK SEARCH ON HYPERCUBE

Hyperspace is one of the early examples, where discrete-time quantum walk search has been implemented [21] to find for a single marked vertex. It has been shown in ref. [30] that two adjacent marked vertices on the hypercube form an *exceptional configuration*, which can not be found using quantum walk search with Grover coin. Here we show that, it is possible to search such *exceptional configuration* on a hypercube by the modified coin \mathcal{C}_G with high success probability.

A n -dimensional hypercube has $N = 2^n$ vertices and n degree. Each vertex is connected to n nearest neighbour vertices. We also attach one self-loop of weight l to each vertex. The Hilbert space of vertices has 2^n dimensions and the edges has $n + 1$ dimensions. A 3-dimensional hypercube is depicted in fig. 6. It has eight vertices and each vertex is connected to three nearest neighbour vertices. The initial state of the coin and vertex space

are

$$|\psi_c^l\rangle = \frac{1}{\sqrt{n+l}} \left(\sum_{x=0}^{n-1} |x\rangle + \sqrt{l} |c_l\rangle \right), \quad (41)$$

$$|\psi_v\rangle = \frac{1}{\sqrt{N}} \sum_{i=0}^{N-1} |v_i\rangle, \quad (42)$$

respectively, where v_i is the binary representation of the decimal number i . For the quantum walk search we start with the initial state $|\psi_{in}\rangle = |\psi_c^l\rangle \otimes |\psi_v\rangle$. The shift operator S moves the walker from a vertex to its n nearest neighbour vertices as

$$|x\rangle |v_i\rangle = |x\rangle |v_i \oplus b_x\rangle, \quad (43)$$

where b_x is the n -bit binary representation of 2^x . For example, in fig. 6, shift operation on the vertex $v_0 = 000$ becomes $S|0\rangle|000\rangle = |0\rangle|000 \oplus 100\rangle = |0\rangle|100\rangle$, $S|1\rangle|000\rangle = |1\rangle|000 \oplus 010\rangle = |1\rangle|010\rangle$ and $S|2\rangle|000\rangle = |2\rangle|000 \oplus 001\rangle = |2\rangle|001\rangle$. Similarly, the shift operator acts on all other vertices of the hypercube as well.

To study the exceptional configuration, let us consider two adjacent marked vertices v_i and $v_i \oplus b_x$, for a specific i, x . We observe that lackadaisical quantum walk has the following stationary state

$$|\psi_{stat}\rangle = |\psi_{in}^l\rangle - \sqrt{\frac{n+l}{N}} (|x\rangle \otimes |v_i\rangle + |x\rangle \otimes |v_i \oplus b_x\rangle). \quad (44)$$

After applying U_l repeatedly t times, the initial state becomes

$$U_l^t |\psi_{in}^l\rangle = |\psi_{stat}\rangle + \sqrt{\frac{n+l}{N}} U_l^t (|x\rangle \otimes |v_i\rangle + |x\rangle \otimes |v_i \oplus b_x\rangle). \quad (45)$$

The first part of eq. (45) does not change. Only the second part evolves under the unitary transformation. The success probability to measure the marked vertices can be found to be $\mathcal{O}(\frac{n}{N})$ for large n . Setting $l = 0$ we obtain the result for the Grover coin discussed in ref. [30].

However, it can be shown that for the \mathcal{C}_{SKW} and \mathcal{C}_G coins the stationary state $|\psi_{stat}\rangle$ becomes non-stationary, leading to high success probability for the pair of adjacent marked vertices on the hypercube.

Experimental results: In fig. 7, success probability to measure a randomly chosen pair of adjacent marked vertices is plotted as a function of the number of iteration steps. We see that success probability for \mathcal{C}_{Grover} and \mathcal{C}_l represented by the green and blue dashed curves respectively does not grow even if we increase the number of iteration steps. However, for \mathcal{C}_{SKW} and \mathcal{C}_G the success probability grows as function of the number of iteration steps represented by the red and cyan dashed curves respectively. However, for the SKW coin we additionally

need to deploy amplitude amplification to further improve the success probability. We observe that *exceptional configurations I* portion of table 1(column 2 with two sub-columns) agrees with the result of a hypercube. Since *exceptional configurations II* do not exist in a hypercube, column 3 of table 1 is not applicable to the hypercube. The experiment is repeated for 10 randomly chosen pairs of adjacent marked vertices with the same experimental setting, which agrees with the result in fig. 7.

V. CONCLUSIONS

Quantum walk algorithm is very much successful in searching for a single marked vertex on various graphs. However, searching for multiple marked vertices on a graph is subject to certain limitations. Two categories of *exceptional configurations*, discussed in this article, are difficult to find by the quantum walk search algorithm with some of the well known coin operators. For example, pair of adjacent vertices can not be found by the Grover coin based quantum walk and lackadaisical quantum walk. There exist more general form of marked vertices in the two-dimensional grid, $k \times 2m$ and $2k \times m$, for k, m being positive integers, which quantum walk search with \mathcal{C}_{Grover} and \mathcal{C}_l coins can not find. Another type of *exceptional configurations*, in which marked vertices are arranged along the diagonal of a square grid and its generalised forms, can not be found by the \mathcal{C}_{SKW} and \mathcal{C}_{Grover} coin based quantum walk search.

However, these *exceptional configurations* can be successfully searched by the quantum walk with \mathcal{C}_G coin. A performance summary of quantum walk search with four different coins presented in table 1, and experimental results presented in figs. 3, 5 and 7 show that \mathcal{C}_G is the only coin, which can successfully search both types of *exceptional configurations*. We also analysed *exceptional configurations I* on a hypercube by numerically evaluating the success probability to measure the marked states for four coin operators, showing that \mathcal{C}_G can search marked vertices. Note that, although we have only considered *exceptional configurations* in this article, except fig. 4, \mathcal{C}_G coin works for other types of configuration of marked vertices as well.

We observe that, the occurrence of *exceptional configurations* in some of the quantum walk search algorithms is not a quantum phenomenon. It is merely a limitation of the associated coin operators, which can be avoided by a suitable choice of coin operator.

We have also studied the non-exceptional configurations of the form $k \times m$, k, m being odd, on a two-dimensional grid. Fig. 4 shows that the performance of \mathcal{C}_G coin to search these configurations is better than the \mathcal{C}_l coin over the variation of the self-loop weight.

One of the limitations of our numerical approach is that we implemented the action of the coin and shift operators on the quantum state in the numerical simulations,

which generally requires exponential resources as pointed out in ref. [31]. It prevents us to increase the size of the graphs beyond a certain point because of the limitations of the computing power. The numerical method combined with analytical method allowed ref. [31] to analyse the time complexity for multiple marked vertices(*non-exceptional configuration*) search on large hypercubes. It would be interesting, if we can adopt the analytical approach of refs. [31, 32] to study *exceptional configurations* with \mathcal{C}_G coin based quantum walk, which can improve our understanding on the searching of *exceptional configurations* in the asymptotic limits.

Another interesting future direction could be to inves-

tigate the performance of \mathcal{C}_G coin to search for marked vertices including *exceptional configurations* on various other graphs and compare the results with the performance of other coin operators.

Data availability Statement: The datasets generated during and/or analysed during the current study are available from the corresponding author on reasonable request.

Conflict of interest: The authors have no competing interests to declare that are relevant to the content of this article.

[1] M. Nielsen and I. Chuang, *Quantum Computation and Quantum Information* (Cambridge University Press, Cambridge, 2000).

[2] L. K. Grover, Pro. 28th Annual ACM Symp. Theor. Comput. (STOC) **212** (1996).

[3] P. R. Giri and V. E. Korepin, Quant. Inf. Process. **16** 1-36 (2017).

[4] P. Benioff, Contemporary Mathematics **305** 112, American Mathematical Society, Providence, RI (2002).

[5] R. Portugal, *Quantum Walks and Search Algorithms*, Springer, New York (2013).

[6] A. M. Childs and J. Goldstone, Phys. Rev. A **70** 022314 (2004).

[7] A. Ambainis, J. Kempe and A. Rivosh, Proceedings 16th Annual ACM-SIAM Symposium Discrete Algorithms, SODA 05, 1099-1108. SIAM, Philadelphia, PA (2005).

[8] N. B. Lovett, M. Everitt, M. Trevers, D. Mosby, D. Stockton and V. Kendon, Nat. Comput. **11** 23-35 (2012).

[9] P. R. Giri and V. E. Korepin, Int. J. of Quant. Inf., Vol. 17, No. 07, 1950060 (2019).

[10] P. R. Giri and V. E. Korepin, Mod. Phys. Lett. A Vol. 33, No. 1 2050043 (2020).

[11] A. M. Childs and J. Goldstone, Phys. Rev. A **70**, 042312 (2004).

[12] S. Chakraborty, L. Novo, A. Ambainis and Yasser Omar, Phys. Rev. Lett. **116**, 100501 (2016).

[13] D. A. Meyer and T. G. Wong, Phys. Rev. Lett. **114** 110503 (2015).

[14] S. Aaronson and A. Ambainis, Theor. Comput. **1(4)** 47-79 (2005).

[15] A. Tulsi, Phys. Rev. A **78** 012310 (2008).

[16] T. G. Wong, J. Phys. A Math. Theor. **48** 43, 435304 (2015).

[17] T. G. Wong, J. Phys. A Math. Theor. **50** 47 475301 (2017).

[18] T. G. Wong, Quant. Inf. Process. **17** 68 (2018).

[19] P. R. Giri, Int. J. Theor. Phys. **62**, 121 (2023).

[20] T. Osada, K. Sanaka, W. J. Munro, and K. Nemoto, Phys. Rev. A **97**, 062319 (2018).

[21] N. Shenvi, J. Kempe, and K. B. Whaley, Phys. Rev. A **67**, 052307 (2003).

[22] N. Nahimovs and A. Rivosh, Proceedings of SOFSEM, **9587** 381-391 (2016).

[23] N. Nahimovs, SOFSEM 2019: Theory and Practice of Computer Science. SOFSEM 2019. Lecture Notes in Computer Science, vol 11376. Springer, Cham (2019).

[24] A. Saha, R. Majumdar, D. Saha, A. Chakrabarti, and S. Sur-Kolay, Quant. Inf. Process. **21**, 275 (2022).

[25] N. Nahimovs and A. Rivosh, Proceedings of the 10th International Doctoral Workshop on Mathematical and Engineering Methods in Computer Science, MEMICS 2015 (Springer, Telč, Czech Republic, 2016) pp. 79-92.

[26] A. Ambainis, A. Rivosh, Proceedings of SOFSEM'08, 485-496, (2008).

[27] M. Li and Y. Shang, New J. Phys. **22** 123030 (2020).

[28] P. R. Giri, Eur. Phys. J. D **77**, 175 (2023).

[29] K. Prūsis, J. Vihrovs, and T. G. Wong, Phys. Rev. A **94** 032334 (2016).

[30] N. Nahimovs and R. Santos, Proceedings of SOFSEM 2017, vol. 10139, pp. 256– 267, (2017).

[31] G. A. Bezerra, P. H. G. Lugão, R. Portugal, Phys. Rev. A **103**, 062202 (2021).

[32] M. Roget, H. Kadri, and G. Di Molfetta, Phys. Rev. Research **5**, 033021 (2023).